

Cooling a strongly-interacting quantum gas by interaction modulation

D. Eberz,¹ A. Kell,¹ M. Breyer,¹ and M. Köhl¹

¹*Physikalisches Institut, University of Bonn, Wegelerstraße 8, 53115 Bonn, Germany*

We present a cooling method for a strongly-interacting trapped quantum gas. By applying a magnetic field modulation with frequencies close to the binding energy of a molecular bound state we selectively remove dimers with high kinetic energy from the sample. We demonstrate cooling of the sample over a wide range of interaction strengths and measure a high cooling efficiency of $\gamma = 4$ that exceeds all previous cooling near Feshbach resonances.

Experiments with trapped ultracold quantum gases have been made possible by groundbreaking advancements in cooling techniques. This has led, for example, to the observation of Bose-Einstein condensation (BEC) [1], degenerate Fermi gases [2] and strongly-correlated quantum states such as Mott insulators [3] and the unitary Fermi gas [4, 5]. Theoretically, many more complex quantum states are expected at even lower temperature, for example, unconventional superconductivity [6], topological quantum states [7] or spin liquids [8]. However, as we approach very low temperatures, efficient cooling becomes increasingly difficult since established cooling methods are limited in reaching even lower temperatures while preserving high densities [9]. This has been a major obstacle on the route to exploring novel phases of matter.

Over the past decades, several techniques to reach even lower temperature have been proposed. This includes, for example, entropy reduction by separating high and low entropy regions in the trap [10–12], by introducing disorder [13], utilizing heat reservoirs in form of a different state or species [14], or by inter-layer entropy exchange in bilayer systems [15]. Novel cooling techniques have been experimentally demonstrated, for example, in the Hubbard model by isolating a low entropy region via potential shaping [16], and by creating site-alternating heat reservoirs via the introduction of a superlattice in one spatial direction [17].

The concept of evaporative cooling is to remove or separate particles with an energy higher than the average energy per particle from the sample. This leads to a reduction of both temperature and atoms, however, when performed efficiently, it will increase the phase-space density and therefore lower the entropy of the gas. This paves the way towards the desired progression towards low-entropy states. In magnetic traps, evaporation is achieved by radio-frequency induced transitions to anti-trapped states and in optical traps by lowering the potential depth. Both methods have been successfully implemented, however, both also have limitations. Evaporative cooling in magnetic traps can be challenging for mixtures of atoms in different spin states, which is a common problem when cooling Fermi gases, and evaporative cooling in optical traps faces the challenge of reducing confinement at the same time as lowering the trap depth. This poses problems for maintaining high densities and staying in the runaway regime of evaporative cooling.

In this work, we demonstrate a novel cooling method

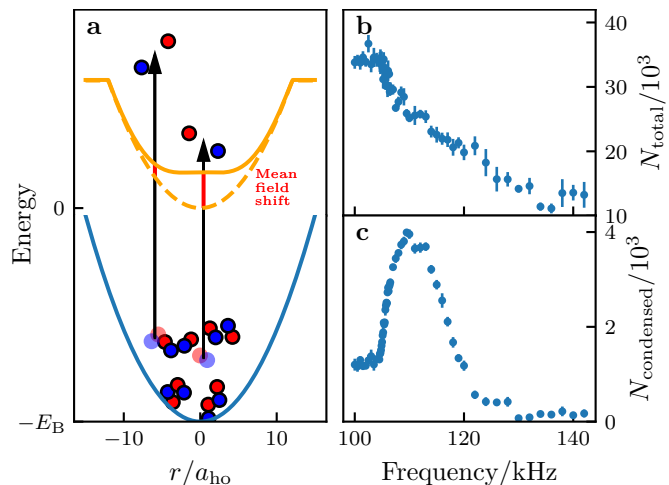


FIG. 1. **a** Composite dimers with binding energy E_B are confined in a harmonic trapping potential (blue line) and constitute a partly condensed quantum gas. A periodic modulation of their interaction strength dissociates them into pairs of fermions with an energy dependent on the modulation frequency and the mean-field energy shift. The latter is proportional to the density of remaining dimers and fermions and introduces a position-dependent dissociation threshold. **b** Varying the modulation frequency leads to evaporation of atoms if the modulation frequency is significantly above the dissociation threshold. **c** If the evaporation is selectively for the dimers with high energies, the number of atoms in the condensate increases contrary to the total decrease of atom number. If the evaporation is non-specific, i.e. far above the dissociation threshold, the condensate is diminished along with the general loss of particles.

for a strongly-interacting quantum gas on the repulsive side of a magnetically-controlled Feshbach resonance. At low temperature the gas comprises of dimers with a binding energy E_B . We apply a time-periodic modulation of the interaction strength with a frequency near to or above the binding energy in order to dissociate dimers with a certain energy and selectively remove them from the sample. The matrix element for the transition depends on the binding energy, the density of states and, last but not least, on the interaction in both initial and final states. We utilize the spatial dependence of the mean-field interaction in a harmonic trapping potential in order to dissociate molecules spatially selectively. This allows us to discriminatively remove particles with an

energy higher than $k_B T$ from the sample. We demonstrate that this method leads to cooling and we show an increase of the condensate fraction of a partially condensed system. Importantly, unlike radio-frequency induced evaporation, our method does not involve a third spin state, thereby eliminating three-body losses, and unlike evaporation in optical dipole traps, it does not soften the trapping potential and slow down thermalization.

Experimentally, we prepare a quantum gas in the lowest and third-lowest hyperfine states $|1\rangle$ and $|3\rangle$ of ^6Li in a crossed-beam optical dipole trap [18] with trap frequencies $(\omega_x, \omega_y, \omega_z) = 2\pi \times (102, 144, 232)$ Hz. We obtain atom numbers of $N_\sigma \sim 5 \cdot 10^4 - 1.5 \cdot 10^5$ per spin state σ at a temperature of $T/T_F \sim 0.1$. The interaction strength and binding energy are adjusted by a magnetically-controlled Feshbach resonance located at 690.43 G with a width of 122.3 G [19]. We calibrate the magnetic field using the $|1\rangle$ to $|2\rangle$ hyperfine transition in a spin-polarised Fermi gas, and the binding energy of the dimer state energy is determined from the magnetic field and the interatomic interaction potential [20–22]. In order to induce pair-breaking excitations, we apply a periodically modulated magnetic field with an amplitude of up to $A_{\text{mod}} \sim 2$ G and a frequency of up to $\nu_{\text{mod}} \sim 300.0$ kHz using a specially designed solenoid [23]. In contrast to a dissociation scheme by radiofrequency modulation [24], the dissociation by magnetic field modulation does not involve transfer to a third hyperfine state and, moreover, does not excite free atoms. After an excitation of usually 300 ms, we introduce a waiting time of 200 ms in order to ensure thermalisation of the sample. During thermalisation, there is a small particle loss since the decay time constant of the condensate is 1 s. Detection is performed by absorption imaging either in-situ or after rapid-ramp projection [4] in time-of-flight.

In Fig. 1a, we show the principle of the cooling scheme. The initial state is a gas predominantly containing dimers in a harmonic potential. Between two dimers, the s-wave scattering length is $a_{\text{dd}} = 0.6a$ [25], where a is the inter-atomic scattering length and this gives rise to the mean-field potential for the dimers $\propto a_{\text{dd}}n$. A time-periodic modulation of the magnetic field at a frequency near the binding energy breaks the dimers into a pair of free atoms. The energy threshold for the dissociation is determined by the dimer binding energy and the difference between initial-state and final-state interactions. The final-state interaction is determined by the scattering length between the dissociated atoms and the remaining dimers, which is $a_{\text{ad}} = 1.18a$ between a dimer and an atom [26]. For modulation frequencies above the dissociation threshold, additional kinetic energy is given to the dissociation fragments, which may evaporate from the trap. The key idea of the cooling scheme is to exploit the change of the mean-field energy before and after dissociation of a dimer into atoms, which is $\delta E = (3a_{\text{ad}} - a_{\text{dd}})2\pi\hbar^2 n_\sigma / m_{\text{Li}}$ [27–29]. As one can see from Fig. 1b, the number of removed particles is a monotonous function of the modulation frequency. The

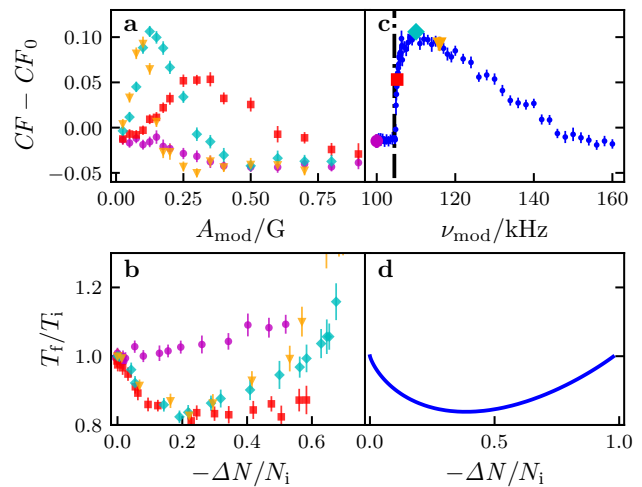


FIG. 2. **a** Change of the condensate (CF) fraction as a function of the modulation amplitude A_{mod} for four different modulation frequencies ν_{mod} of 100.0 kHz (purple, circle), 105.2 kHz (red, square), 110.0 kHz (cyan, diamond) and 116.0 kHz (orange, triangle). The sample has a binding energy of 104.5(5) kHz. **b** Variation of the temperature with the fractional atom loss $-\Delta N/N_i$ for the same modulation amplitudes and frequencies as in **a**. **c** Maximum relative condensate fraction for each driving frequency. The four frequencies from **a** are highlighted in the corresponding colors. The dashed-dotted line shows the binding energy. The error bars show the standard error. **d** Theoretical estimate for the cooling as a function of atom number loss using an interacting Bose gas model, see main text.

dissociation is position sensitive due to the mean-field shift. For low density – which equals high energy of dimers in the trap – the dissociation threshold is close to the binding energy E_B . In contrast, for high densities, the dissociation threshold is shifted due to the mean-field interaction to larger values and more particles are removed from the trap. By explicitly dissociating dimers in the high-energy tails of their Boltzmann distribution, which corresponds to low densities in a harmonic trap, we are able to effectively reduce the energy per particle, cool the sample, and enhance the phase-space density, see Figure 1c.

In Fig. 2a we show the change of condensate fraction due to the periodic modulation of the magnetic field with respect to modulation strength and modulation frequency at a magnetic field of 640.31(6) G, corresponding to a binding energy of 104.5(5) kHz. We observe distinct regimes of cooling and heating depending on frequency and modulation amplitude. For a modulation at or below the frequency of the binding energy we observe no increase in condensate fraction, but instead the condensate decays with increasing modulation strength. In Fig. 2b we show the corresponding change of the temperature of the gas, which, again, shows the regimes of cooling and heating as above. For a more meaningful comparison later, the modulation amplitude axis is replaced by

the corresponding atom loss $-\Delta N/N_i$, with respect to the initial atom number N_i . For each modulation frequency we determine the maximum achieved condensate fraction and plot an overview of all maxima in Fig. 2c. We notice that cooling is possible over a wide range of modulation frequencies above the energy corresponding to the binding energy.

We also have investigated how rapid the cooling method works. The data of Figure 2 are for a modulation time of 300 ms for which we can systematically study a broad range of modulation amplitudes. If we instead focus on the strongest possible modulation amplitude, we can significantly shorten the cooling time. To this end, we have determined that the modulation time to achieve maximum cooling scales as $t_{\text{mod}} \propto 1/\sqrt{A_{\text{mod}}}$ and we can achieve the same peak increase of the condensate fraction as in Figure 2 with a cooling time of $t_{\text{mod}} = 9.3$ ms, followed by a $1/e$ thermalisation time of ~ 20 ms.

In order to explain our cooling scheme and the dependence of the cooling effect on the modulation frequency, we have developed a simplified model based on the step model of evaporative cooling [30]. We describe the initial density distribution of the dimers by a trapped interacting Bose gas. To this end, we employ our independently measured atom number, temperature (see below), and trap frequencies, and we compute the internal energy for the initial state. As the cooling step, we remove a certain fraction (depending on the modulation frequency) of dimers from the sample, and, finally, we compute the internal energy and temperature of the remaining dimers. For the comparison between the model and our data, we focus on the fractional atom loss $-\Delta N/N_i$ and show that we can reach a 15% reduction of the initial temperature for a fractional atom loss of 30%. The magnitude of the cooling effect is in agreement with the experimental observations in Fig. 2b. In the experimental data, we actually also observe heating for certain parameter regimes. This effect is not captured by our model and could be caused by several reasons: Firstly, not all dissociated dimers will leave the trapping region but some could remain with excess kinetic energy from above-threshold dissociation. Secondly, our model ignores the dimer condensate and dissociation from the dimer condensate removes over-proportionally many dimers with zero kinetic energy.

In order to quantify the cooling efficiency, we additionally measure the phase-space density versus atom number at the modulation parameters corresponding to maximum enhancement of the condensate fraction. To this end, we take high-intensity absorption images [31] of the sample to reconstruct the 3D density profile $n_\sigma(r)$ per spin state via the inverse Abel transformation [32]. We use the density at the trap center $n \equiv n_\sigma(r=0)$ for the phase-space-density $\tilde{\rho} = n\lambda_{\text{dB}}^3$, with λ_{dB} being the thermal de-Broglie wavelength. In order to determine the temperature, we fit the outer wings of the reconstructed density profile to the virial expansion of the equation of state [33]. In Figure 3a we show the reduced temper-

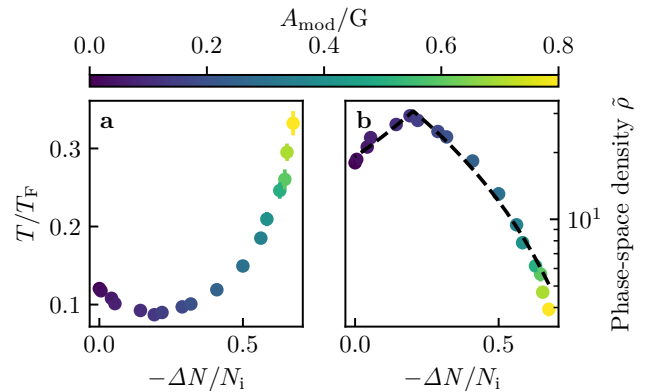


FIG. 3. Cooling of a sample with binding energy 104.5(5) kHz at a modulation frequency of 110.0 kHz. The colorbar highlights the applied modulation amplitude. **a** Shows the atom number with respect to the reduced temperature after cooling. **b** Phase-space density vs. the atom number in a logarithmic plot. The dashed line displays the piece-wise exponential fit to determine the cooling efficiency. Errorbars are standard errors and might be hidden by datapoints.

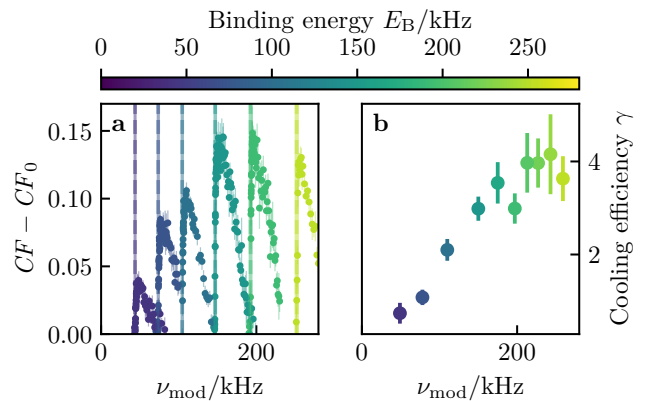


FIG. 4. Cooling of samples from the bosonic side of the BEC/BCS crossover towards unitarity. The position in the crossover is given by the binding energy E_B in the color map. **a** Maximum gain of the condensate fraction as determined in Fig. 2b. The vertical dashed lines show the binding energy for the chosen magnetic field. **b** Cooling efficiency as determined in Fig. 3b.

ature T/T_F and in Figure 3b the phase-space-density $\tilde{\rho}$ with respect to the fractional atom loss $-\Delta N/N_i$ at an exemplary magnetic field of 640.31(6) G (the same as in Figure 2c) and a modulation frequency of 110.0 kHz. For small modulation amplitudes we observe a reduction of temperature and an increase of phase-space density and for high modulation amplitude, the fractional atom loss overwhelms the cooling effect leading to heating.

The efficiency of evaporative cooling is measured by the parameter $\gamma = -\log(\tilde{\rho}_f/\tilde{\rho}_i)/\log(N_{\sigma,f}/N_{\sigma,i})$ [30], which is a metric of how much the phase-space den-

sity increases $\tilde{\rho}_i \rightarrow \tilde{\rho}_f$ while reducing the atom number $N_{\sigma,i} \rightarrow N_{\sigma,f}$. To deduce the cooling efficiency γ we fit a piece-wise exponential function with the efficiency as the exponent to the data, which can be seen as curves in the logarithmic plot in Figure 3b. A positive slope indicates the regime of efficient cooling and a negative slope a regime that should be avoided for evaporation. The maximum efficiency for a given binding energy depends on both modulation frequency and amplitude. In the samples with large binding energy, say $E_B \sim 200$ kHz, we reach an efficiency of $\gamma \sim 4$, which matches or exceeds the best reported values of γ in magnetic and optical traps [30, 34–37].

In Figure 4, we show how the cooling works as we vary the binding energy all the way from the bosonic side of the BEC/BCS crossover to unitarity. Generally, we observe that cooling works best for deeply-bound dimers and the efficiency reduces when approaching the unitarity regime. Figure 4a shows the maximum change of the condensate fraction as determined in Fig. 2c, and Figure 4b shows the maximum cooling efficiency. For the lowest magnetic fields, i.e. the largest binding energy, we observe an increase of the condensate fraction by ~ 0.15 and a cooling efficiency of ~ 4 . Getting closer to the unitary regime the cooling becomes less and eventually, at an

interaction parameter of $1/(k_F a) \sim 0.7$, the condensate fraction does not increase and the cooling efficiency drops below unity. There are at least two effects, which contribute to this behaviour: Firstly, a small dimer binding energy makes the excitation less spatially selective, and, secondly, with the increasing dimer size towards the unitary regime many-body correlations play an increasingly important role, which changes the spectral line shape of the excitation [38].

While the results of the manuscript have been shown for a gravity tilted trap in a $|1\rangle$ - $|3\rangle$ mixture, we observe cooling in a gravity-compensated trap and for a $|1\rangle$ - $|2\rangle$ mixture with comparable efficiency. Hence, the cooling method should be ready to implement in a large variety of systems.

In conclusion, we demonstrate a novel cooling scheme for a gas in the BEC/BCS crossover regime based on the targeted removal of high energy atoms from an optical trap by dimer dissociation. Samples can be cooled without changing the trap geometry which simplifies staying in the run-away regime and to reach very high efficiencies.

This work has been supported by the Deutsche Forschungsgemeinschaft through SFB/TR 185 (project B4) and the Cluster of Excellence Matter and Light for Quantum Computing (ML4Q) EXC 2004/1 – 390534769.

-
- [1] M. H. Anderson, J. R. Ensher, M. R. Matthews, C. E. Wieman, and E. A. Cornell, Observation of Bose-Einstein Condensation in a Dilute Atomic Vapor, *Science* **269**, 198 (1995).
- [2] B. DeMarco and D. S. Jin, Onset of Fermi Degeneracy in a Trapped Atomic Gas, *Science* **285**, 1703 (1999).
- [3] M. Greiner, O. Mandel, T. Esslinger, T. W. Hänsch, and I. Bloch, Quantum phase transition from a superfluid to a Mott insulator in a gas of ultracold atoms, *Nature* **415**, 39 (2002).
- [4] C. A. Regal, M. Greiner, and D. S. Jin, Observation of Resonance Condensation of Fermionic Atom Pairs, *Physical Review Letters* **92**, 040403 (2004).
- [5] J. Kinast, S. L. Hemmer, M. E. Gehm, A. Turlapov, and J. E. Thomas, Evidence for Superfluidity in a Resonantly Interacting Fermi Gas, *Physical Review Letters* **92**, 150402 (2004).
- [6] M. Sigrist and K. Ueda, Phenomenological theory of unconventional superconductivity, *Rev. Mod. Phys.* **63**, 239 (1991).
- [7] A. Y. Kitaev, Unpaired majorana fermions in quantum wires, *Physics-Uspekhi* **44**, 131 (2001).
- [8] J. Knolle and R. Moessner, A field guide to spin liquids, *Annual Review of Condensed Matter Physics* **10**, 451 (2019).
- [9] E. Timmermans, Degenerate Fermion Gas Heating by Hole Creation, *Physical Review Letters* **87**, 240403 (2001).
- [10] M. Popp, J.-J. Garcia-Ripoll, K. G. Vollbrecht, and J. I. Cirac, Ground-state cooling of atoms in optical lattices, *Physical Review A* **74**, 013622 (2006).
- [11] B. Capogrosso-Sansone, S. G. Söyler, N. Prokof'ev, and B. Svistunov, Monte Carlo study of the two-dimensional Bose-Hubbard model, *Physical Review A* **77**, 015602 (2008).
- [12] J.-S. Bernier, C. Kollath, A. Georges, L. De Leo, F. Gerbier, C. Salomon, and M. Köhl, Cooling fermionic atoms in optical lattices by shaping the confinement, *Physical Review A* **79**, 061601 (2009).
- [13] F. N. Ünal and E. J. Mueller, Cooling quantum gases with entropy localization, *New Journal of Physics* **19**, 023045 (2017).
- [14] T.-L. Ho and Q. Zhou, Squeezing out the entropy of fermions in optical lattices, *Proceedings of the National Academy of Sciences* **106**, 6916 (2009).
- [15] A. Kantian, S. Langer, and A. Daley, Dynamical Disentangling and Cooling of Atoms in Bilayer Optical Lattices, *Physical Review Letters* **120**, 060401 (2018).
- [16] C. S. Chiu, G. Ji, A. Mazurenko, D. Greif, and M. Greiner, Quantum State Engineering of a Hubbard System with Ultracold Fermions, *Physical Review Letters* **120**, 243201 (2018).
- [17] B. Yang, H. Sun, C.-J. Huang, H.-Y. Wang, Y. Deng, H.-N. Dai, Z.-S. Yuan, and J.-W. Pan, Cooling and entangling ultracold atoms in optical lattices, *Science* **369**, 550 (2020).
- [18] A. Behrle, T. Harrison, J. Kombe, K. Gao, M. Link, J.-S. Bernier, C. Kollath, and M. Köhl, Higgs mode in a strongly interacting fermionic superfluid, *Nature Physics* **14**, 781 (2018).
- [19] G. Zürn, T. Lompe, A. N. Wenz, S. Jochim, P. S. Julienne, and J. M. Hutson, Precise Characterization of Li 6 Feshbach Resonances Using Trap-Sideband-Resolved RF Spectroscopy of Weakly Bound Molecules, *Physical Re-*

- view Letters **110**, 135301 (2013).
- [20] B. Gao, Binding energy and scattering length for diatomic systems, *Journal of Physics B: Atomic, Molecular and Optical Physics* **37**, 4273 (2004).
- [21] G. F. Gribakin and V. V. Flambaum, Calculation of the scattering length in atomic collisions using the semiclassical approximation, *Physical Review A* **48**, 546 (1993).
- [22] J. Mitroy and M. W. J. Bromley, Semiempirical calculation of van der Waals coefficients for alkali-metal and alkaline-earth-metal atoms, *Physical Review A* **68**, 052714 (2003).
- [23] A. Kell, M. Link, M. Breyer, A. Hoffmann, M. Köhl, and K. Gao, A compact and fast magnetic coil for the manipulation of quantum gases with Feshbach resonances, *Review of Scientific Instruments* **92**, 093202 (2021).
- [24] S. Gupta, Z. Hadzibabic, M. W. Zwierlein, C. A. Stan, K. Dieckmann, C. H. Schunck, E. G. M. van Kempen, B. J. Verhaar, and W. Ketterle, Radio-Frequency Spectroscopy of Ultracold Fermions, *Science* **300**, 1723 (2003).
- [25] D. S. Petrov, C. Salomon, and G. V. Shlyapnikov, Weakly Bound Dimers of Fermionic Atoms, *Physical Review Letters* **93**, 090404 (2004).
- [26] G. V. Skorniakov and K. A. Ter-Martirosian, Three Body Problem for Short Range Forces. I. Scattering of Low Energy Neutrons by Deuterons, *Soviet Phys. JETP* **Vol: 4** (1957).
- [27] R. Combescot, A. Recati, C. Lobo, and F. Chevy, Normal State of Highly Polarized Fermi Gases: Simple Many-Body Approaches, *Physical Review Letters* **98**, 180402 (2007).
- [28] S. Giorgini, L. P. Pitaevskii, and S. Stringari, Theory of ultracold atomic Fermi gases, *Reviews of Modern Physics* **80**, 1215 (2008).
- [29] L. P. Pitaevskii and S. Stringari, *Bose-Einstein condensation and superfluidity*, first edition ed., International series of monographs on physics No. 164 (Oxford University Press, Oxford, United Kingdom, 2016).
- [30] W. Ketterle and N. V. Druten, Evaporative Cooling of Trapped Atoms, in *Advances In Atomic, Molecular, and Optical Physics*, Vol. 37 (Elsevier, 1996) pp. 181–236.
- [31] K. Hueck, N. Luick, L. Sobirey, J. Siegl, T. Lompe, H. Moritz, L. W. Clark, and C. Chin, Calibrating high intensity absorption imaging of ultracold atoms, *Optics Express* **25**, 8670 (2017).
- [32] Y. Shin, M. W. Zwierlein, C. H. Schunck, A. Schirotzek, and W. Ketterle, Observation of Phase Separation in a Strongly Interacting Imbalanced Fermi Gas, *Physical Review Letters* **97**, 030401 (2006).
- [33] M. Link, K. Gao, A. Kell, M. Breyer, D. Eberz, B. Rauf, and M. Köhl, Machine Learning the Phase Diagram of a Strongly Interacting Fermi Gas, *Physical Review Letters* **130**, 203401 (2023).
- [34] S. R. Granade, M. E. Gehm, K. M. O’Hara, and J. E. Thomas, All-Optical Production of a Degenerate Fermi Gas, *Physical Review Letters* **88**, 120405 (2002).
- [35] A. J. Olson, R. J. Niffenegger, and Y. P. Chen, Optimizing the efficiency of evaporative cooling in optical dipole traps, *Physical Review A* **87**, 053613 (2013).
- [36] R. Roy, A. Green, R. Bowler, and S. Gupta, Rapid cooling to quantum degeneracy in dynamically shaped atom traps, *Physical Review A* **93**, 043403 (2016).
- [37] J.-F. Clément, J.-P. Brantut, M. Robert-de Saint-Vincent, R. A. Nyman, A. Aspect, T. Bourdel, and P. Bouyer, All-optical runaway evaporation to Bose-Einstein condensation, *Physical Review A* **79**, 061406 (2009).
- [38] C. H. Schunck, Y.-i. Shin, A. Schirotzek, and W. Ketterle, Determination of the fermion pair size in a resonantly interacting superfluid, *Nature* **454**, 739 (2008).